The Role of Ligand Binding in the Kinetic Folding Mechanism of Human $p21^{H-ras}$ Protein†

Jing Zhang and C. Robert Matthews*

Department of Chemistry and Center for Biomolecular Structure and Function, The Pennsylvania State University, University Park, Pennsylvania 16802

Received May 13, 1998; Revised Manuscript Received August 24, 1998

ABSTRACT: $p21^{H-ras}$ plays a critical role in signal transduction pathways by cycling between an active, GTP/Mg^{2+} ternary complex and an inactive, GDP/Mg^{2+} complex. Urea-induced equilibrium unfolding studies [Zhang and Matthews (1998) *Biochemistry 37*, 14881−14890] have shown that GDP and Mg^{2+} play essential roles in stabilizing the protein. To probe the mechanism of folding and to examine the effects of these ligands on the kinetic folding reaction, unfolding and refolding experiments were performed at a variety of urea and ligand concentrations. A burst phase intermediate with substantial secondary structure and marginal stability was observed during refolding by stopped-flow circular dichroism spectroscopy. Three subsequent refolding phases were detected using a combination of absorbance, circular dichroism, and fluorescence spectroscopy. The fastest phase involves ligand binding and appears to directly form the fully folded enzyme. The intermediate and slow phases do not depend on either urea or ligand concentration under strongly refolding conditions and appear to reflect isomerization or rearrangement reactions. Double- jump experiments demonstrated that the intermediate and slow refolding phases both lead to the native conformation and correspond to parallel rather than sequential reactions. Unfolding is controlled by two phases that involve the release of the ligands when the ligands are in excess. At stoichiometric ligand concentrations, however, the rate-limiting steps in unfolding change from ligand release to isomerization or rearrangement reactions at high urea concentrations. Only the faster unfolding reaction is observed in the absence of Mg^{2+}, suggesting that this reaction corresponds to the unfolding of the binary complex, $p21^{H-ras}$•GDP. The slower unfolding reaction presumably corresponds to the unfolding of the ternary complex, $p21^{H-ras}$•GDP•Mg^{2+}. The kinetic data show that the refolding/unfolding of $p21^{H-ras}$ occurs through parallel channels that are strongly influenced by the binding/release of GDP and Mg^{2+} to/from a pair of native conformers.

Many proteins require noncovalently bound ligands or cofactors to perform their biological functions. Hydrolysis, radical generation, electron transfer, group transfer, photochemical energy conversion, regulation of gene expression, and oxidation−reduction, among other reactions, can be mediated by a variety of extrinsic cofactors that greatly expand the repertoire of cellular processes executed by polypeptides.

The essential role of such factors in function has prompted investigations into their role in folding and stability (*1*−*5*). For example, the removal of calcium from α-lactalbumin induces a molten globule state under conditions that favor the native conformation (*6*−*8*). This partially folded form is very similar to a transient intermediate that appears in the first few milliseconds of folding in the presence of calcium (*6*). Studies on carp parvalbumin (*4*) and bovine carbonic anhydrase (*9*, *10*) have shown that metal ions can facilitate folding reactions. Thus, tightly bound ligands not only may stabilize the native conformation but also may accelerate the folding reactions that lead to its formation.

A particularly interesting example of a protein whose function is controlled by extrinsic ligands is $p21^{H-ras}$.[1] This enzyme is a member of the GTPase superfamily whose guanine nucleotide binding pocket is highly conserved among the GTP binding proteins (*11*−*15*). $p21^{H-ras}$ plays a central role in signal transduction by cycling between the active, GTP-bound, and inactive, GDP-bound, conformations (*16*). Mutation at any one of the positions 12, 13, or 61 leads to oncogenesis (*17, 18*) by stabilizing the protein in its GTP-bound conformation. As a consequence, $p21^{H-ras}$ has been the target of many drug discovery and clinical studies (*19*, *20*).

Several structures of the truncated form of $p21^{H-ras}$ (residues 1−166), complexed with various ligands, have been determined (*21*−*27*). This protein is a member of the α/β-sheet class of proteins, with five α-helices and a central β-sheet which contains five parallel and one antiparallel

† This work was supported by NSF Grant MCB 9604678 to C.R.M.

* To whom correspondence should be addressed.

[1] Abbreviations: ABS, absorbance; β-ME, β-mercaptoethanol; CD, circular dichroism; FL, fluorescence; GDP, guanosine diphosphate; GTP, guanosine triphosphate; Na_2EDTA, ethylenediaminetetraacetic acid, disodium salt; $NaDodSO_4$, sodium dodecyl sulfate; $NADP^+$, nicotinamide adenine dinucleotide phosphate, oxidized form; PAGE, polyacrylamide gel electrophoresis; $p21^{H-ras}$, p21 protein product of the H-ras gene; SF, stopped-flow; Tris, tris(hydroxymethyl)aminomethane; UV, ultraviolet.

10.1021/bi981116z CCC: $15.00
Published on Web 10/02/1998

strands [Figure 1 in (*28*)]. Of the 10 loops, 5 contribute side chain and backbone interactions essential to the binding of the nucleotide and metal ion.

The reversible, urea-induced equilibrium unfolding of $p21^{H-ras}$, bound to GDP and Mg^{2+}, has been found to be well described by a two-state model involving the native ternary complex and the unfolded protein from which the ligands have been released (*28*). Comparison of the ternary complex and the apo protein demonstrated that GDP and Mg^{2+} induce the formation of well-defined tertiary structure and dramatically increase the stability of the protein. The present study probes the role of these ligands in the kinetic folding mechanism of $p21^{H-ras}$.

MATERIALS AND METHODS

Protein Source and Purification. Full-length $p21^{H-ras}$ was expressed in *Escherichia coli* JM105 cells containing the TACHRAS plasmid (a gift from John H. Coulby). The protein was purified according to previously published procedures (*29*) with some modifications (*28*). The purity of the protein was verified by the presence of a single band on Coomassie blue-stained $NaDodSO_4$−polyacrylamide gels. Apo $p21^{H-ras}$ was prepared by unfolding the ternary complex in buffer containing 6 M urea and passage over a Sephadex G-25 column to remove the ligands and denaturant, as previously described (*28*).

Reagents and Experimental Conditions. Ultrapure urea was purchased from ICN Biomedical, Inc. (Costa Mesa, CA); GDP was purchased from Sigma (St. Louis, MO), and $MgCl_2$ was purchased from Aldrich Chemical Co., Inc. (Milwaukee, WI). All other chemicals were reagent grade. The buffer used in all folding experiments contained 20 mM Tris-HCl, pH 7.5, 67−100 mM NaCl, 2 mM β-ME, and appropriate $MgCl_2$ and GDP concentrations. The concentration of NaCl was varied between 67 and 100 mM to maintain a constant total ionic strength equivalent to 120 mM (including buffer) when the concentrations of Mg^{2+} and Na_2EDTA were varied. The temperature was maintained at 25 °C for all experiments. Samples were prepared by dialysis against the folding buffer at 4 °C.

Kinetic Folding Studies. Kinetic data for folding reactions whose relaxation times exceeded 10 s were obtained by manual mixing techniques. Changes in the secondary structure of $p21^{H-ras}$ as a function of time following changes in urea concentration were monitored by far-UV circular dichroism spectroscopy at 222 nm with an AVIV 62DS spectrometer. Mean residue ellipticity was calculated using an average residue molecular mass of 112.2 g mol^{-1}. Slow changes in tertiary structure were monitored by absorbance spectroscopy at 287 nm with an AVIV 14DS UV−Vis spectrometer. Fast folding reactions (τ < 10 s) were monitored by stopped-flow fluorescence using a Biologic SFM-3 fluorometer and by CD spectroscopy using a Biologic SFM-3 drive-train interfaced to the AVIV 62DS. In both cases, the optical path length was 2 mm, and the deadtime of mixing was 5 ms (*30*). For the fluorescence experiments, the excitation wavelength was 275 nm and the slit width was 10 nm. The emission was monitored at wavelengths greater than 295 nm with a cutoff filter provided by Biologic.

Double-Jump Experiments. Double-jump experiments (unfolded → native → unfolded) were performed in the following manner. $p21^{H-ras}$ was initially unfolded in folding buffer (20 mM Tris-HCl, pH 7.5, 85 mM NaCl, 5 mM $MgCl_2$, 100 μM GDP, 2 mM β-ME) containing 6 M urea overnight at a concentration of 100 μM to avoid aggregation of the unfolded protein. The sample was then concentrated on a Centricon-3 (Amicon), using a molecular mass cutoff of 3000 Da, to a final concentration of 600 μM. Refolding was initiated by manually mixing 20 μL of unfolded protein with 180 μL of folding buffer to give a final urea concentration of 0.6 M at 25 °C. After various refolding times from 30 s to 50 min, 60 μL samples were withdrawn and manually mixed with 540 μL of folding buffer containing 9 M urea to give a final urea concentration of 8.2 M. The unfolding kinetics were monitored by the decrease in ellipticity at 222 nm using CD spectroscopy. The amplitudes of the two unfolding phases were obtained by analyzing the kinetic response for each unfolding experiment as the sum of two exponentials.

Kinetic Data Analysis. To simplify the analysis of the kinetic data, refolding reactions were primarily performed under pseudo-first-order conditions with respect to the ligand concentrations; i.e., the concentrations of GDP and Mg^{2+} were at least 10-fold higher than the protein concentration. Both the refolding and unfolding kinetic data were fit to a sum of exponentials:

$$A(t) = A(\infty) + \sum A_i \exp(-t/\tau_i)$$

where $A(t)$ and $A(\infty)$ are the total amplitude at time t and the amplitude at infinite time, respectively. A_i and τ_i are the amplitude and the relaxation time for the ith component of the fit. The data were fit using either a commercially available, nonlinear least-squares program, NLIN (SAS Institute Inc., Cary, NC), or an in-house global fitting program, Savuka version 5.0. Similar results were obtained with both fitting procedures.

Burst Phase Analysis. The stability of the burst phase intermediate was estimated from the dependence of the ellipticity at 222 nm after 5 ms on the final urea concentration. The urea dependence of the burst phase amplitude was fit to a two-state model using equations described in the preceding paper (*28*). The calculation of the stability of the burst phase intermediate involved the assumption that the unfolded baseline region was well-described by that observed for the unfolded apo protein and the unfolded ternary complex. The native baseline was fit assuming a linear dependence on denaturant concentration (*31*).

RESULTS

Kinetics of the Unfolding Reaction. The loss of secondary and tertiary structure during the unfolding of $p21^{H-ras}$ was monitored by far-UV CD and near-UV absorbance spectroscopies, respectively. In the presence of 100 μM GDP and 5 mM Mg^{2+}, the complete unfolding of $p21^{H-ras}$ at 8 M urea and 25 °C monitored by CD requires more than 8 h (Figure 1A); similar results were obtained from measurement of the absorbance at 287 nm (data not shown). The unfolding traces obtained by both CD and absorbance spectroscopies were well fit by two exponentials whose relaxation times were designated τ_{u1} and τ_{u2}. By varying the final urea concentration, it was found that the relaxation times of both the slower, τ_{u1}, and faster, τ_{u2}, phases decrease exponentially

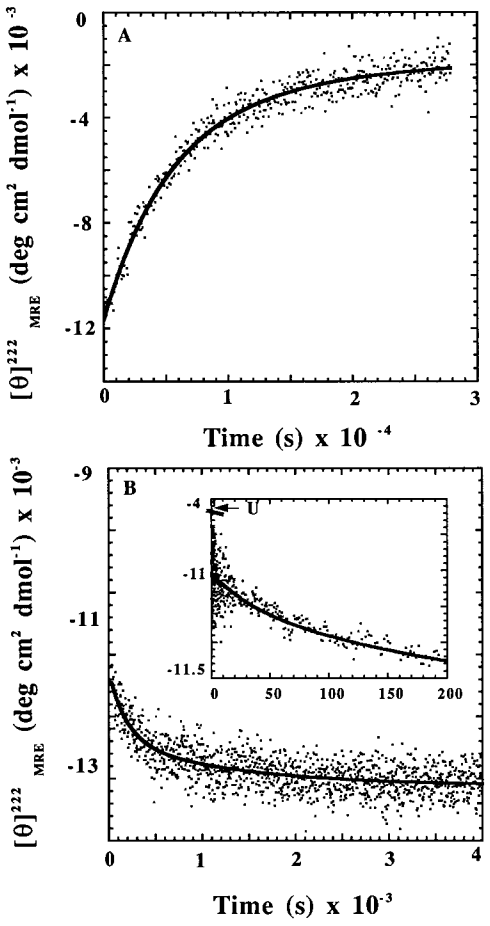

FIGURE 1: Time dependence of the mean residue ellipticity changes at 222 nm for the unfolding and refolding of p21^{H-ras}. (A) Unfolding from 0 to 8 M urea, at pH 7.5 and 25 °C, as monitored by manual mixing CD. The final GDP, Mg^{2+}, and protein concentrations were 100 μM, 5 mM, and 10 μM, respectively. (B) Refolding from 6 to 0.6 M urea at the same final ligand and protein concentrations as in (A). The insert shows the fast refolding reaction monitored by stopped-flow CD. The arrow indicates the expected initial mean residue ellipticity of p21^{H-ras} unfolded in 0.6 M urea and was calculated from equilibrium CD studies (*28*). The buffer contained 20 mM Tris-HCl, pH 7.5, 25 °C, 85 mM NaCl, and 2 mM β-ME.

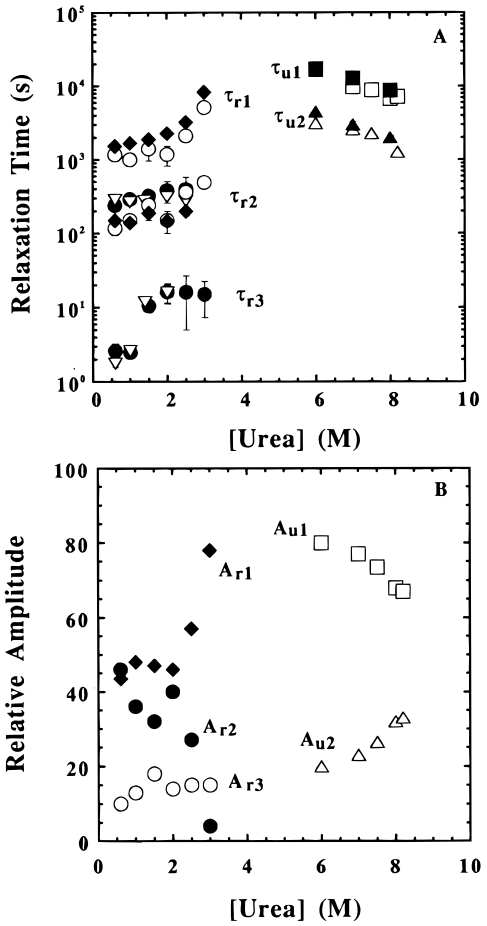

FIGURE 2: (A) Urea dependence of the unfolding and refolding relaxation times at pH 7.5, 25 °C. Refolding data were obtained from manual mixing CD (open circles), SF-CD (closed circles), SF-FL (open reversed triangles), and manual mixing UV absorbance (closed diamonds). Unfolding data were obtained from manual mixing CD (open squares and triangles) and UV absorbance (closed squares and triangles). (B) Urea dependence of the unfolding and refolding amplitudes obtained by CD spectroscopy at pH 7.5, 25 °C. The fast, intermediate, and slow folding phases are designated by open circles, closed circles, and closed diamonds, respectively. The fast and slow unfolding phases are designated by open triangles and squares, respectively. Ligand and protein concentrations as well as buffer conditions are described in the caption to Figure 3.

with increasing urea concentration (Figure 2A). This behavior is typical of protein unfolding reactions (*32*) and implies that the rate-limiting steps in unfolding of p21^{H-ras} involve substantial changes in the buried surface area (*33*, *34*). The excellent agreement in the magnitudes of the relaxation times detected by these two optical techniques (Figure 2A) demonstrates that secondary and tertiary structure are disrupted in a concerted fashion.

The amplitudes of kinetic phases contain useful information about the concentrations of the initial species in a folding reaction (*35*). At 6 M urea, the relative amplitudes of the τ_{u1} and τ_{u2} phases detected by CD spectroscopy are 80% and 20%, respectively, of the total signal (Figure 2B). As the urea concentration is increased, the relative amplitude of the slower, τ_{u1}, phase decreases while that for the faster, τ_{u2}, phase increases. The total change in mean residue ellipticity at 222 nm accounted for by these two phases is 10 310 $\pm$ 1032 deg cm^2 dmol^{-1}, within error of the value expected from equilibrium studies, 11 182 deg cm^2 dmol^{-1} (Figure 3, and (*28*). The good agreement demonstrates that no significant fast unfolding reaction occurs under these conditions.

Kinetics of the Refolding Reaction. Stopped-flow CD refolding experiments showed that about 60−70% of the ellipticity at 222 nm appears in less than 5 ms, consistent with the formation of a burst phase intermediate (Figure 1B, inset). The subsequent increase in signal was well-described by three exponential phases. Under strongly refolding conditions, 0.6 M urea, the relaxation times of the τ_{r1}, τ_{r2}, and τ_{r3} phases are 1200 $\pm$ 56 s, 200 $\pm$ 12 s, and 3 $\pm$ 0.6 s, respectively. Very similar results were obtained by a combination of stopped-flow fluorescence and manual mixing absorbance spectroscopy, demonstrating that both secondary structure and tertiary structure develop in all folding phases.

The dependencies of the refolding relaxation times of the three observable refolding phases on the urea concentration are shown in Figure 2A. Note that limitations in the signal-to-noise ratio precluded observation of the τ_{r3} phase by stopped-flow absorbance, and instrumental drift precluded accurate measurement of the τ_{r1} phase by stopped-flow fluorescence. The relative amplitudes obtained from CD

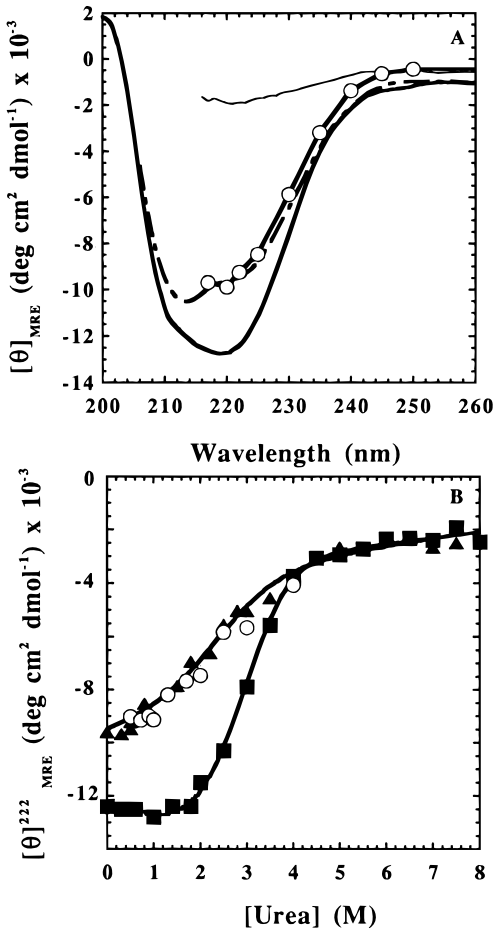

FIGURE 3: (A) Far-UV CD spectra of the burst phase intermediate (open circles), the ternary complex, p21^{H-ras}·GDP·Mg^{2+} (solid line), and the apo p21^{H-ras} (broken line) in 0.6 M urea; the ternary complex in 8 M urea is also shown (thin solid line). (B) Mean residue ellipticity at 222 nm versus urea concentration for the burst phase intermediate (open circles), the ternary complex (closed squares), and the apo p21^{H-ras} (closed triangles). The data for the apo protein and ternary complex were taken from (*28*). Solid lines indicate fits to a two-state equilibrium unfolding model. The buffer contained 20 mM Tris-HCl, pH 7.5, 25 °C, 85 mM NaCl (for the ternary complex and the burst phase intermediate) or 100 mM NaCl (for the apo protein), and 2 mM β-ME. The final concentrations for the ternary complex and apo protein were 16.5 and 10 μM, respectively.

spectroscopy, where all three phases could be detected by a single technique, are shown in Figure 2B. The relaxation time of the fastest, τ_{r3}, refolding phase increases with increasing final urea concentrations up to 2 M urea and appears to be independent of the denaturant concentration between 2 and 3 M urea. The relative amplitude of this phase, which represents approximately 15% of the total signal (neglecting the burst phase reaction), does not depend strongly on denaturant. The relaxation time of the τ_{r2} phase does not depend significantly on the urea concentration, suggesting that this phase corresponds to an isomerization or rearrangement reaction with a small change in the buried surface area (*36*). The relative amplitude of this phase, however, decreases monotonically as the urea increases. The complex urea dependence for the relaxation time of the slowest, τ_{r1}, phase suggests that a folding reaction is limiting above 2 M urea and an isomerization or rearrangement reaction is limiting below 2 M urea. Between 2 and 3 M urea, the amplitude of the τ_{r1} reaction increases with a concomitant amplitude decrease for the τ_{r2} reaction; the τ_{r1} phase dominates the observed change in ellipticity at 3 M urea.

Attempts to test for a proline isomerization reaction by catalysis with the prolyl isomerase cyclophilin (*37*) were unsuccessful. The refolding of p21^{H-ras} at 5 °C, where cyclophilin has optimal activity (*38*, *39*), is extremely slow. Under these conditions, p21^{H-ras} tends to aggregate (unpublished data).

Structure and Stability of the Burst Phase Intermediate. The far-UV CD spectrum of the burst phase intermediate was obtained by measuring the burst phase amplitude at different wavelengths and the same final urea concentration, 0.6 M (Figure 3A). For comparison, the far-UV CD spectra of the ternary complex and the apo forms of p21^{H-ras} in the same solvent are also shown in Figure 3A. Between 216 and 250 nm, the spectrum of the burst phase intermediate is very similar to that of apo p21^{H-ras} (*28*). The residual urea in the refolding buffer precluded accurate measurements below 216 nm. At 222 nm, the mean residue ellipticities of the burst phase species and the apo protein are -9.3×10^3 and -9.5×10^3 deg cm^2 dmol^{-1}, respectively. The folded, ternary complex exhibits a minimum at 220 nm, typical of α/β-sheet proteins, and has a mean residue ellipticity at 222 nm of -12.3×10^3 deg cm^2 dmol^{-1}. From these data, it is clear that a substantial fraction of the secondary structure, perhaps as much as 75%, develops within the deadtime of the kinetic experiment, 5 ms. The similarity of the far-UV CD spectrum of the apo protein and that of the burst phase species suggests that these partially folded forms have similar compositions of secondary structure.

The stability of the burst phase species was determined by measuring the CD signal at 222 nm after 5 ms at a series of final urea concentrations. The dependence of the mean residue ellipticity attributed to the burst phase species on the urea concentration is shown in Figure 3B. The dependencies of the mean residue ellipticity for the ternary and apo p21^{H-ras} on the urea concentration are also shown in Figure 3B for comparison. The near-coincidence of the unfolding transition curves for the burst phase intermediate and apo p21^{H-ras} demonstrates that these species have similar stabilities. Assuming a two-state unfolding model, the free energies of unfolding in the absence of denaturant, $\Delta G°(H_2O)$, for the burst phase and apo species are 1.6 ± 0.2 kcal mol^{-1} and 1.8 ± 0.2 kcal mol^{-1}, respectively. Both species are marginally stable compared to the ternary complex which has a free energy of unfolding of 14.1 kcal mol^{-1} under standard state conditions (*28*).

The parameter describing the dependence of the Gibbs free energy on the concentration of denaturant, the *m* value, is also nearly identical for two forms of p21^{H-ras}: $m = 0.73 \pm 0.02$ kcal mol^{-1} (molar urea)$^{-1}$ for the burst phase intermediate and 0.78 ± 0.02 kcal mol^{-1} (molar urea)$^{-1}$ for the apo protein. The near-equivalence of the *m* values suggests that both forms have a similar amount of buried surface area (*36*). Given that the *m* value for the ternary complex is 1.37 mol^{-1} (molar urea)$^{-1}$ (*28*), the buried surface areas for both apo p21^{H-ras} and the burst phase intermediate are approximately 55% that for the ternary complex, p21·GDP·Mg^{2+}.

Effects of Ligands on the Unfolding Reactions of p21^{H-ras}. To determine the influence of GDP and Mg^{2+} on the two unfolding phases observed for p21^{H-ras}, unfolding was carried

Table 1: Relative Amplitudes and Relaxation Times of the Unfolding Phases of P21^{H-ras} in 8 M Urea as a Function of Ligand Concentration at pH 7.5 and 25 °C

[GDP][a] (μM)	[Mg^{2+}] (mM)	A_1[c] (%)	A_2[c] (%)	τ_{u1}[c] (s)	τ_{u2}[c] (s)
10	0.0001[b]	0	100	–	20
10	0.010	50	50	64	25
10	5.010	95	5	3140	790
50	0.010	70	30	91	22
110	0.0001[b]	0	100	–	30
110	5.010	78	22	10200	1990

[a] [GDP] is the total concentration in the solution. The protein concentration was 10 μM for all experiments. [b] [Mg^{2+}] is the concentration in solution when 5 mM Mg^{2+} and 10 mM Na_2EDTA were present. [c] Errors are estimated to be ±10%.

out at several ligand concentrations (Table 1). For 10 μM p21^{H-ras} in the presence of 110 μM GDP and 5 mM Mg^{2+}, two very slow phases are observed by CD spectroscopy. At 8 M urea, τ_{u1} and τ_{u2} are 10 200 and 1990 s, respectively. When the Mg^{2+} concentration is decreased, these two phases are greatly accelerated. When 10 μM p21^{H-ras} is unfolded with 50 μM GDP and 10 μM Mg^{2+} at 8 M urea, τ_{u1} and τ_{u2} are 91 and 22 s, respectively. When the GDP concentration was decreased from 50 to 10 μM, while maintaining the Mg^{2+} concentration at 10 μM, the relaxation time of the two unfolding phases did not change significantly.

The role of Mg^{2+} in these unfolding reactions was further highlighted by preincubating p21^{H-ras} with an excess of Na_2EDTA to form the binary complex. When 10 mM Na_2EDTA was present in the unfolding buffer along with either 10 μM or 110 μM GDP and 5 mM Mg^{2+}, only a single unfolding phase was observed. The relaxation times in 8 M urea were 20 and 30 s, respectively, similar to the faster of the two phases observed with stoichiometric ligands present, 25 s. The total amplitude change for this reaction in the presence of 10 mM Na_2EDTA was equal to that obtained in the absence of Na_2EDTA (data not shown), indicating that the complete unfolding reaction was observed in both cases.

Although both unfolding relaxation times decrease exponentially at increasing urea concentration with excess ligands (Figures 2A and 4), the situation is more complex at stoichiometric ligand concentrations (Figure 4). Up to approximately 4 M urea, both reactions accelerate with increasing urea concentration. Above 4 M urea, both relaxation times appear to approach constant values when equimolar protein and ligands are present. The same behavior is observed for the single unfolding reaction observed in the presence of excess Na_2EDTA (Figure 4).

The relative amplitudes of the two unfolding phases were also found to be dependent on the concentrations of GDP and Mg^{2+} (Table 1). As the concentration of either ligand concentration is increased, the relative amplitude of the slower, τ_{u1}, phase increases with a concomitant decrease in the amplitude of the faster, τ_{u2}, phase. The dependence of these amplitudes on the ligand concentrations suggests that a preexisting equilibrium between two native or nativelike conformers may exist.

Effect of Ligands on the Refolding Reactions of p21^{H-ras}. To examine the effect of GDP and Mg^{2+} on the rates of the refolding reaction, refolding jumps were performed at a series of final ligand concentrations under strongly refolding

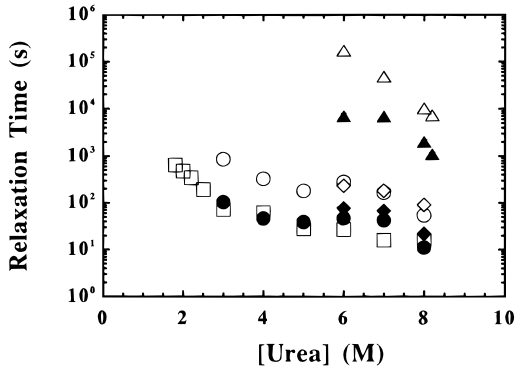

FIGURE 4: Urea dependence of the unfolding relaxation times from far-UV CD spectroscopy as a function of the final ligand concentrations. The open and closed triangles represent the relaxation times of the two phases obtained for 10 μM p21^{H-ras} in the presence of 110 μM GDP and 5 mM Mg^{2+}; the open and closed circles are the relaxation times of the two unfolding phases obtained in the presence of stoichiometric ligands; i.e., the final GDP and Mg^{2+} concentrations were 10 μM; the open and closed diamonds represent the relaxation times of the two unfolding phases obtained in the presence of 50 μM GDP and 10 μM Mg^{2+}; and the open squares are those obtained in the presence of 5 mM Mg^{2+} and 10 mM Na_2EDTA; i.e., the final GDP and Mg^{2+} concentrations were 10 and 0.1 μM, respectively. The buffer contained 20 mM Tris-HCl, pH 7.5, 25 °C, 85 mM NaCl (for the ternary complex and the burst phase intermediate) or 100 mM NaCl (for the apo protein), and 2 mM β-ME.

conditions. The response was monitored by absorbance, stopped-flow fluorescence, and stopped-flow circular dichroism spectroscopies. The absence of an effect on the burst phase CD amplitude (data not shown) suggests that neither Mg^{2+} nor GDP binds to the burst phase intermediate, consistent with the comparable CD spectra observed for the burst phase intermediate and the apo protein (Figure 3). The relaxation time of the fastest, τ_{r3}, phase decreases when the concentration of either GDP or Mg^{2+} is increased (Figure 5), demonstrating that this reaction involves ligand binding. By contrast, the intermediate, τ_{r2}, phase and the slow, τ_{r1}, phases do not depend on GDP or Mg^{2+} concentrations (Figure 5).

The ligand dependence on refolding from 6 to 2.5 M urea, where folding and not isomerization begins to be the limiting reaction, was examined by kinetic refolding jumps at a series of final Mg^{2+} and GDP concentrations. No measurable ligand dependence was found for the two slow refolding phases under marginal folding conditions (data not shown).

Double-Jump Experiments. Double-jump experiments can be used to distinguish between the appearance of native and partially folded forms by monitoring the amplitude of unfolding phases as a function of the delay between the refolding and subsequent unfolding jumps (*40*, *41*). Using manual mixing far-UV CD spectroscopy, protein unfolded in 6 M urea was refolded by dilution to 0.6 M urea. After various delay times, the protein was subsequently unfolded to 8.2 M urea. Two unfolding phases with relaxation times of 1400 and 5600 s at 8.2 M urea appear over delay times ranging from 30 s to 50 m. These relaxation times are very similar to those for the unfolding of the native p21^{H-ras} under the same final conditions, indicating that these two reactions reflect the unfolding of native p21^{H-ras}. The amplitudes of the two phases as a function of delay time are plotted in Figure 6. The amplitude of the faster unfolding phase is

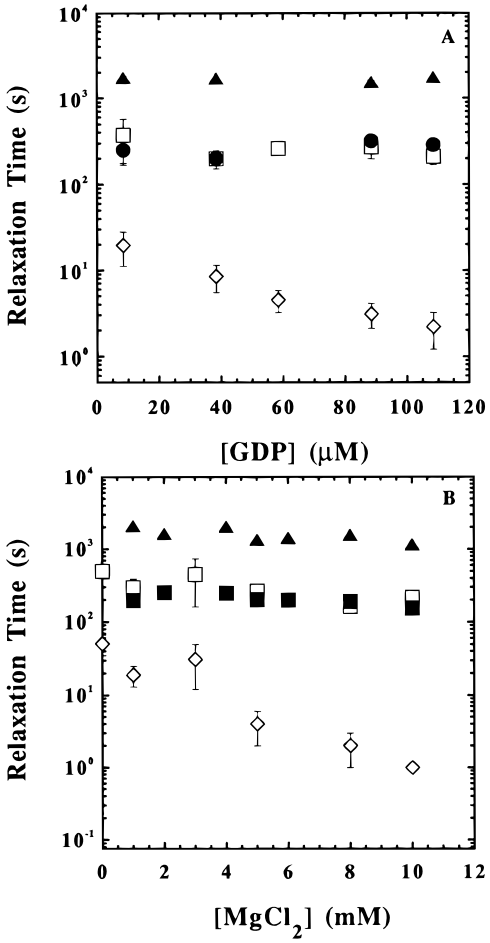

FIGURE 5: Ligand dependence of the refolding relaxation times for $p21^{H-ras}$. (A) Relaxation times vs GDP concentration. The Mg^{2+} and protein concentrations were maintained constant at 5 mM and 8.4 μM, respectively. The buffer contained 20 mM Tris-HCl, at pH 7.5, 25 °C, 85 mM NaCl, and 2 mM β-ME. (B) Relaxation times vs Mg^{2+} concentration. The GDP and protein concentrations were maintained constant at 100 and 8.4 μM, respectively. Open symbols represent data obtained from SF-CD, and closed symbols represent data from manual mixing CD. The buffer contained 20 mM Tris-HCl, at pH 7.5, 25 °C, 100−70 mM NaCl (according to the final Mg^{2+} concentration), and 2 mM β-ME.

1.4×10^3 deg cm^2 dmol^{-1} after a minimum delay of 30 s, proceeds through a maximum around 500 s, and then decreases slightly to the value observed for fully folded protein. The slower unfolding phase has an amplitude of 0.8×10^3 deg cm^2 dmol^{-1} after 30 s and progressively increases to its maximum value after 1000 s. As discussed below, these results support the notion that each of the three refolding phases can lead directly to native $p21^{H-ras}$.

DISCUSSION

Model for the Kinetic Unfolding Reaction. A kinetic model for the unfolding of $p21^{H-ras}$ that can explain the complex dependence of this reaction on ligand and denaturant concentrations is shown in Scheme 1.

N_1·GDP·Mg^{2+} is a folded, ternary complex, N_2·GDP is a folded, binary complex, I_1·GDP·Mg^{2+} is an intermediate, ternary complex, I_2·GDP is an intermediate, binary complex, and U is the ensemble of unfolded forms that does not bind ligands.

Under conditions favoring the native form of $p21^{H-ras}$, the ternary complex, N_1·GDP·Mg^{2+}, is the predominant conformer in the presence of saturating GDP and Mg^{2+} (*28*, *42*). When challenged with high concentrations of denaturant, this species undergoes an isomerization or structural rearrangement reaction to I_1·GDP·Mg^{2+} whose buried surface area is similar to that of N_1·GDP·Mg^{2+}. After the isomerization reaction, the intermediate ternary complex then unfolds and releases the ligands. The transient response of this sequential pair of reactions is reflected in the τ_{u1} unfolding phase. The observation of another, faster unfolding phase, τ_{u2}, which has a similar dependence on denaturant and ligand concentrations as the τ_{u1} phase and which persists in the presence of Na_2EDTA, suggests that the binary complex, N_2·GDP, and a corresponding intermediate, I_2·GDP, are also involved in the unfolding of $p21^{H-ras}$.

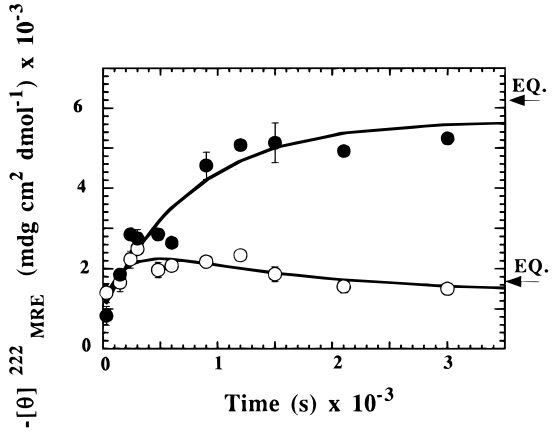

FIGURE 6: Dependence of the amplitudes of the slow (filled circles) and fast (open circles) unfolding phases on the delay time between refolding and unfolding jumps for $p21^{H-ras}$. The refolding buffer contained 0.6 M urea and 20 mM Tris-HCl, at pH 7.5, 25 °C, 85 mM NaCl, 5 mM $MgCl_2$, 100 μM GDP, and 2 mM β-ME. The final protein concentration was 6.0 μM. Lines are drawn to aid the eye.

Scheme 1: Model for the Kinetic Unfolding of $p21^{H-ras}$

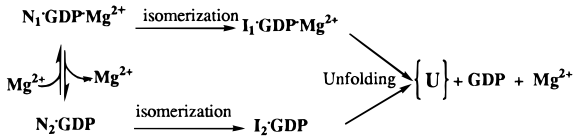

Both isomerization and unfolding steps contribute to the observed relaxation times, but the rate-limiting step depends on the ligand and denaturant concentrations. At high ligand concentrations, the stabilization of the native and intermediate forms relative to U causes the unfolding, ligand-release reaction to be rate-limiting at all accessible urea concentrations. When the ligand concentrations are decreased, unfolding is accelerated to the point that isomerization or rearrangement reactions become rate-limiting at high urea concentrations in both channels. The approach of a folding relaxation time to a constant value as a function of urea has been described as a rollover effect (*43*).

The placement of the isomerization reactions before the global unfolding reactions in both channels is based upon the observation that only two phases are detected under all conditions. If unfolding preceded isomerization, four phases would be expected under strongly unfolding conditions and stoichiometric ligand concentration. Note that the proposed isomerization reaction in the τ_{u2} channel cannot be the conversion of the ternary to the binary complex because the

same isomerization reaction is observed in the absence of Mg^{2+} (Figure 4). This interconversion reaction must accelerate as the ligand concentrations are decreased to explain the existence of two unfolding phases across a time scale ranging from 1000−10 000 to 10−100 s for these reactions.

The choice of a parallel rather than sequential set of kinetic steps for τ_{u1} and τ_{u2} is based upon the observation that both unfolding phases display a similar dependence on denaturant and ligand concentration. Parallel unfolding reactions are also consistent with the observation of a single phase in the presence of Na_2EDTA and with the independent development and subsequent unfolding of a pair of native conformers detected by the double-jump experiment (see below).

A surprising feature of this model is the proposal that the binary complex, N_2·GDP, plays a significant role in the unfolding of the ternary complex. Previous measurements of the affinity of GDP for $p21^{H-ras}$ in the presence and absence of Mg^{2+} (*42*) and of the stabilities of the ternary and binary complexes (*28*) imply that, in the absence of denaturant, the equilibrium between these two forms greatly favors the ternary complex. However, the urea dependence of the relative free energies of unfolding of the binary and ternary complexes is such that the free energy of the binary complex begins to approach that of the ternary complex at high urea concentration. This coalescence results from the greater *m* value for the more completely folded ternary complex. As a result, the 6.6 kcal mol^{-1} difference in free energies between the binary and ternary forms in the absence of denaturant decreases to 3.6 kcal mol^{-1} at 8.2 M urea. Therefore, although the binary, N_2·GDP, complex is predicted to be the minor species under unfolding conditions, its 10-fold faster rate of unfolding could permit a significant fraction of protein to unfold through this form. The decrease in the free energy difference between the native binary and ternary complexes is also consistent with the increase in the amplitude of the faster unfolding reaction with increasing urea concentration (Figure 2B).

The model also can account for the increase in the relative amplitude of the slow unfolding phase at increasing ligand concentrations (Table 1). The enhanced affinity of GDP for $p21^{H-ras}$ in the presence of excess Mg^{2+} (*42*, *44*, *45*) implies that increasing the concentration of either ligand will shift the equilibrium between N_1·GDP·Mg^{2+} and N_2·GDP to favor the ternary complex. As a result, a larger fraction of the protein should unfold via the slower, τ_{u1}, reaction.

Model for the Kinetic Refolding Reaction. The complex response observed in the absorbance, far-UV CD, and fluorescence signals during the refolding of $p21^{H-ras}$ implies that multiple species are involved. These results, along with those from the double-jump experiment (Figure 6), permit the formulation of a kinetic model for the refolding reaction.

Within 5 ms, the manifold of rapidly interconverting unfolded forms of $p21^{H-ras}$ fold to a set of burst phase intermediates designated I_{BP}^{F}, $I_{BP}^{1/S}$, and $I_{BP}^{2/S}$. I_{BP}^{F} is a partially folded form that can rapidly and directly fold to either of the native conformers, N_1·GDP·Mg^{2+} and N_2·GDP, while binding the appropriate ligands. The relaxation times for these events are proposed to be similar and be reflected in the τ_{r3} reaction. $I_{BP}^{1/S}$ and $I_{BP}^{2/S}$ are partially folded forms that must isomerize or rearrange their structures to I_1 and I_2, respectively, before becoming competent to bind ligands and fold to their respective native conformers. These sequential reactions are reflected in the τ_{r1} and τ_{r2} refolding phases. The interconversions between these three burst phase forms and between the subsequent intermediates are sufficiently slow that folding within each channel is favored over folding between channels. The binary native complex, N_2·GDP, then binds Mg^{2+} to form the more stable, ternary complex, N_1·GDP·Mg^{2+}.

The rollover behavior observed for the τ_{r1} phase (Figure 2) suggests that the rate-limiting step switches from folding to isomerization as the urea concentration decreases. The lack of the dependence of the τ_{r1} relaxation time on ligand concentration under conditions where either the isomerization reaction or the folding reaction in this channel is at least partially limiting, 2.5 M urea, suggests that GDP and Mg^{2+} only bind to the native conformation. The existence of a refolding reaction for the τ_{r2} phase can only be inferred from the behavior of the τ_{r1} phase because the amplitude of the τ_{r2} phase approaches zero at 2.5 M urea.

The existence of three burst intermediates and the formulation of the later steps in the refolding model are based primarily on the results of the double-jump experiment. The appearance of 10−15% of the amplitude in each of the two unfolding reactions within 30 s of the initiation of refolding (Figure 6) is most easily explained by postulating that the τ_{r3} refolding phase represents a pair of reactions with similar relaxation times that link a burst phase intermediate, I_{BP}^{F}, with the two native conformations responsible for these unfolding phases, N_1·GDP·Mg^{2+} and N_2·GDP. The sensitivity of the τ_{r3} relaxation time to ligand concentration (Figure 5) is consistent with ligand binding in the transition states for these two reactions. The observation of only a single relaxation time for the τ_{r3} phase as the Mg^{2+} concentration is increased, although only the channel leading to N_1·GDP·Mg^{2+} is proposed to bind Mg^{2+}, may reflect the preferred partitioning of I_{BP}^{F} into this channel by Mg^{2+}.

The reappearance of additional amplitude for the faster, τ_{u2}, unfolding phase in the double-jump experiment over the first 500 s (Figure 6) suggests that the species corresponding to this unfolding reaction is the product of the τ_{r2} refolding reaction. The relaxation time of the τ_{r2} reaction is ∼250 s during the refolding incubation step (Figure 2). Using a similar argument, the reappearance of the amplitude in the τ_{u1} unfolding phase in the first few thousand seconds of folding suggests that the native species associated with this unfolding phase is primarily the product of the τ_{r1} refolding reaction.

If the τ_{r2} and τ_{r1} reactions were sequential, the 4−5-fold difference in the τ_{r1} and τ_{r2} refolding relaxation times would result in a substantial buildup and then complete dissipation of the species responsible for the τ_{u2} unfolding reaction (*46*). Because this behavior is not observed, it is more likely that the τ_{r1} and τ_{r2} reactions occur simultaneously in parallel channels. The small decrease in the amplitude of the τ_{u2} reaction between 500 and 3000 s, however, suggests that some of the protein that folds through the τ_{r2} reaction reequilibrates with the product of the τ_{r1} reaction. Apparently, the partitioning of $p21^{H-ras}$ into various folding channels is at least partially kinetically controlled (*47*).

Given the formation of the two native forms through parallel channels, the lack of proportionality between the relative rate constants for the τ_{r1}, τ_{r2}, and τ_{r3} phases and the relative amplitudes (Figure 2) shows that a minimum of three

burst phase intermediates must exist. Proportional amplitudes are predicted for a mechanism in which a single species partitions into multiple product forms (*46*). The three burst phase forms, I_{BP}^{F}, $I_{BP}^{1/S}$, and $I_{BP}^{2/S}$, are predicted to have significant secondary structure (Figure 3A) and similar but marginal stability (Figure 3B). These characteristics suggest that these intermediates may be similar to molten globules, partially folded forms that have been observed to appear in the folding of other proteins (*6*, *48*). In the case of $p21^{H-ras}$, the resemblance of these early intermediates to the folded apo protein (Figure 3A) is consistent with ligand binding at later stages in folding.

The dependence of the relative amplitudes of the τ_{r1} and τ_{r2} refolding phases on the final urea concentration (Figure 2B) suggests that $I_{BP}^{1/S}$ and $I_{BP}^{2/S}$ persist for a sufficient time to allow a reequilibration of these two species. By contrast, I_{BP}^{F} folds more rapidly than reequilibration can occur with the slower folding intermediates. The increase in amplitude for the τ_{r1} phase and the concomitant decrease in the amplitude of the τ_{r2} phase at increasing final urea concentration are consistent with greater stability for the intermediate associated with the formation of the ternary complex, $I_{BP}^{1/S}$. The lack of dependence of the τ_{r3} phase on the final urea concentration may imply that the I_{BP}^{F} intermediate folds before such a linkage can be established.

The ligand-independent isomerization reactions observed in the refolding of $p21^{H-ras}$ for the τ_{r1} and τ_{r2} phases (Figure 2A) are unlikely to be proline isomerization reactions (*49*). cis proline isomers are generally minor species in peptides and, presumably, unfolded proteins. Therefore, unless a prolyl peptide bond is cis in the native conformation, the cis/trans isomerization reaction would not be expected to limit the folding of a majority of the refolding protein. Given that all six proline peptide bonds in $p21^{H-ras}$ are in the trans form, the observation that the two isomerization reactions each account for approximately 40% of the refolding protein requires that another explanation must be sought for these reactions.

An attractive alternative is the possibility is that subdomain/subdomain rearrangement reactions are involved. When the manifold of unfolded forms collapses into either I_{BP}^{F}, $I_{BP}^{1/S}$, or $I_{BP}^{2/S}$, the distinguishing feature between these early intermediates may be the way in which two (or more) subdomains dock on each other. Non-native "complexes" would be required to rearrange to forms that can then undergo large-scale folding reactions to the native conformation, e.g., the τ_{r1} and τ_{r2} folding phases. Nativelike "complexes" would be able to directly fold to the native conformation, i.e., the τ_{r3} folding phase.

Support for this explanation can be found in the redistribution of the amplitudes of the τ_{r1} and τ_{r2} phases at increasing final urea concentration (Figure 2B). This result is consistent with a urea-sensitive equilibrium between $I_{BP}^{1/S}$ and $I_{BP}^{2/S}$ that could correspond to the interconversion of two partially folded forms with alternative packing of two subdomains.

The Role of Ligand Binding in the Folding of $p21^{H-ras}$. The unfolding and refolding models presented in Schemes 1 and 2, respectively, postulate that GDP and/or Mg^{2+} only bind to native or very nativelike species. The only refolding reaction that is sensitive to ligand concentration, the τ_{r3} reaction, was shown to lead directly to the native conformation by the double-jump experiment. By contrast, both of the rate-limiting steps in unfolding depend on the ligand concentrations when the ligands are in excess. Only when the ligands are present at stoichiometric or lower concentrations are ligand-independent isomerization reactions limiting at high denaturant concentration.

Scheme 2: Model for the Kinetic Refolding of $p21^{H-ras}$

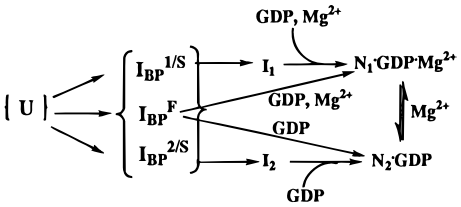

These results can be understood in terms of the distributed nature of the ligand binding sites across the amino acid sequence of $p21^{H-ras}$. GDP directly interacts with the backbone and side chains from eight different segments of the protein. Mg^{2+} binds to the β-phosphate of GDP and to Ser17 in helix 1. Therefore, the late binding of these ligands is a likely consequence of the necessity to bring multiple segments of the protein into proper juxtaposition for binding. Apparently, the required backbone and side chain placements only occur at or very near the final stage of folding when the native conformation appears. According to this argument, the transition state for the τ_{r3} reaction is also very nativelike since it appears to be able to bind the ligands.

Similar conclusions were reached previously for a set of calcium binding proteins (*4*, *5*, *50*). The acceleration of the folding of α-lactalbumin (*50*) and parvalbumin (*4*) by Ca^{2+} but the absence of an effect on staphylococcal nuclease (*5*) demonstrated that Ca^{2+} binds to folding intermediates in the two albumins but only to the native conformation of the nuclease. These results were interpreted to mean that the sequence proximity of the chelating side chains in α-lactalbumin and parvalbumin makes it possible for Ca^{2+} to bind to a partially folded form. The greater separation of the chelating side chains in the nuclease sequence, similar to $p21^{H-ras}$, precludes ligand binding until the native conformation is reached.

Therefore, although GDP and Mg^{2+} play critical roles in the stability and folding of $p21^{H-ras}$, these ligands do not exert their influence until the final stage of folding. The polypeptide contains sufficient information and inherent stability to drive the folding reaction to a set of molten globule-like forms that strongly resemble the apo protein. The acquisition of most of the stability and the development of the tertiary structure require the binding of GDP and Mg^{2+} to a binding site that is distributed across the amino acid sequence of $p21^{H-ras}$.

Biological Implications. For $p21^{H-ras}$ to act effectively as a molecular switch in signal transduction pathways, it must exist in the inactive, GDP-bound state for a period of time which is comparable to or longer than the events stimulated by the active, GTP-bound state (*14*). One fundamental limit on the lifetime of the inactive state is determined by the rate of ligand release that accompanies the unfolding of $p21^{H-ras}$. From the data presented in Table 1 and Figures 2 and 4, the relaxation time for unfolding of the ternary complex in the absence of urea can be estimated to exceed 10^4 s at 25 °C. This value is about 10-fold longer than the observed exchange rate of the GDP-bound form (*14*, *51*), demonstrat-

ing that the intrinsic exchange reaction does not require global unfolding. The nucleotide exchange factors that catalyze this reaction by up to 100-fold (*14*, *51*) may act to enhance the local unfolding reactions that are apparently responsible for ligand exchange.

ACKNOWLEDGMENT

We are grateful to Dr. S. Campbell-Burk for the gift of the gene of $p21^{H-ras}$ and the purification protocol for this protein. We thank Drs. J. A. Zitzewitz, V. F. Smith, and L. M. Gloss for their critical reviews of the manuscript and S. A. Wasta for her assistance with references.

REFERENCES

1. Yazgan, A., and Henkens, R. W. (1972) *Biochemistry 11*, 1314−1318.
2. Lin, L.-N., and Brandts, J. F. (1978) *Biochemistry 17*, 4102−4110.
3. Ikeguchi, M., Kuwajima, K., Mitani, M., and Sugai, S. (1986) *Biochemistry 25*, 6965−6972.
4. Kuwajima, K., Sakuraoka, A., Fueki, S., Yoneyama, M., and Sugai, S. (1988) *Biochemistry 27*, 7419−7428.
5. Sugawara, T., Kuwajima, K., and Sugai, S. (1991) *Biochemistry 30*, 2698−2706.
6. Kuwajima, K. (1989) *Proteins: Struct., Funct., Genet. 6*, 87−103.
7. Creighton, T. E., and Ewbank, J. J. (1994) *Biochemistry 33*, 1534−1538.
8. Kuwajima, K. (1996) *FASEB J. 10*, 102−109.
9. Kiefer, L. L., and Fierke, C. A. (1994) *Biochemistry 33*, 15233−15240.
10. Aronsson, G., Martensson, L. G., Carlsson, U., and Jonsson, B.-H. (1995) *Biochemistry 34*, 2153−2162.
11. Halliday, K. R. (1983) *J. Cyclic Nucleotide Protein Phosphorylation Res. 9*, 435−448.
12. McCormick, F., Clark, B. F. C., LaCour, T. F. M., Kjeldgaard, M., Norskov-Lauritsen, L., and Nyborg, J. (1985) *Science 230*, 78−82.
13. Dever, T. E., Glynias, M. J., and Merrick, W. C. (1987) *Proc. Natl. Acad. Sci. U.S.A. 84*, 1814−1818.
14. Bourne, H. R., Sanders, D. A., and McCormick, F. (1991) *Nature 349*, 117−127.
15. Valencia, A., Kjeldgaard, M., Pai, E. F., and Sander, C. (1991) *Proc. Natl. Acad. Sci. U.S.A. 88*, 5443−5447.
16. Barbacid, M. (1987) *Annu. Rev. Biochem. 56*, 779−827.
17. Balmain, A., and Pragnell, I. B. (1983) *Nature 303*, 72−74.
18. Zarbl, H., Sukumar, S., Arthur, A. V., Martin-Zanca, D., and Barbacid, M. (1985) *Nature 315*, 382−385.
19. Pavlovic, J., Shroder, A., Blank, A., Pitoss, F., and Staeheli, P. (1993) in *Ciba Foundation Symposium*, pp 233−247, Wiley, Chichester.
20. Hall, A. (1994) *Science 264*, 1413−1414.
21. Pai, E. F., Krengel, U., Petsko, G. A., Goody, R. S., Kabsch, W., and Wittinghofer, A. (1990) *EMBO J. 9*, 2351−2359.
22. Schlichting, I., Almo, S. C., Rapp, G., Wilson, K., Petratos, K., Lentfer, A., Wittinghofer, A., Kabsch, W., Pai, E. F., Petsko, G. A., and Goody, R. S. (1990) *Nature 345*, 309−315.
23. Milburn, M. V., Tong, L., de Vos, A. M., Brunger, A., Yamaizumi, Z., Nishimura, S., and Kim, S.-H. (1990) *Science 247*, 939−945.
24. Tong, L., de Vos, A. M., Milburn, M. V., and Kim, S. H. (1991) *J. Mol. Biol. 217*, 503−516.
25. Goody, R. S., Pai, E. F., Schlichting, I., Rensland, H., Scheidig, A., Franken, S., and Wittinghofer, A. (1992) *Philos. Trans. R. Soc. London 336*, 3−10.
26. Kraulis, P. J., Domaille, P. J., Campbell-Burk, S. L., Van Aken, T., and Laue, E. D. (1994) *Biochemistry 33*, 3515−3531.
27. Scheidig, A. J., Franken, S. M., Corrie, J. E., Reid, G. P., Wittinghofer, A., Pai, E. F., and Goody, R. S. (1995) *J. Mol. Biol. 253*, 132−150.
28. Zhang, J., and Matthews, C. R. (1998) *Biochemistry 37*, 14881−14890.
29. DeLoskey, R. J., Van Dyk, D. E., Van Aken, T. E., and Campbell-Burk, S. (1994) *Arch. Biochem. Biophys. 311*, 72−78.
30. Mann, C. J., and Matthews, C. R. (1993) *Biochemistry 32*, 5282−5290.
31. Santoro, M. M., and Bolen, D. W. (1988) *Biochemistry 27*, 8063−8068.
32. Matthews, C. R. (1987) *Methods Enzymol. 154*, 498−511.
33. Schellman, J. A. (1978) *Biopolymers 17*, 1305−1322.
34. Kuwajima, K., and Schmid, F. X. (1984) *Adv. Biophys. 18*, 43−74.
35. Tanford, C. (1968) *Adv. Protein Chem. 23*, 218−282.
36. Myers, J. K., Pace, C. N., and Scholtz, J. M. (1995) *Protein Sci. 4*, 2138−2148.
37. Fischer, G., Wittmann-Liebold, B., Lang, K., Kiefhaber, T., and Schmid, F. X. (1989) *Nature 337*, 476−478.
38. Weisman, R., Creanor, J., and Fantes, P. (1996) *EMBO J. 15*, 447−456.
39. Yoo, S., Myszka, D. G., Yeh, C., McMurray, M., Hill, C. P., and Sundquist, W. I. (1997) *J. Mol. Biol. 269*, 780−795.
40. Schmid, F. X. (1981) *Eur. J. Biochem. 114*, 105−109.
41. Schmid, F. X., and Blaschek, H. (1981) *Eur. J. Biochem. 114*, 111−117.
42. John, J., Sohmen, R., Feuerstein, J., Linke, R., Wittinghofer, A., and Goody, R. S. (1990) *Biochemistry 29*, 6058−6065.
43. Baldwin, R. L. (1996) *Folding Des. 1*, R1−R8.
44. Feuerstein, J., Kalbitzer, H. R., John, J., Goody, R. S., and Wittinghofer, A. (1987) *Eur. J. Biochem. 162*, 49−55.
45. Mistou, M.-Y., Cool, R. H., and Parmeggiani, A. (1992) *Eur. J. Biochem. 204*, 179−185.
46. Bernasconi, C. F. (1976) *Relaxation Kinetics*, Academic Press, New York.
47. Jennings, P. A., Finn, B. E., Jones, B. E., and Matthews, C. R. (1993) *Biochemistry 32*, 3783−3789.
48. Ptitsyn, O. B. (1994) *Protein Eng. 7*, 593−596.
49. Brandts, J. F., Halvorson, H. R., and Brennan, M. (1975) *Biochemistry 14*, 4953−4963.
50. Kuwajima, K., Mitani, M., and Sugai, S. (1989) *J. Mol. Biol. 206*, 547−561.
51. Mosteller, R. D., Han, J., and Broek, D. (1994) *Mol. Cell. Biol. 14*, 1104−1112.

BI981116Z